Intense foreshocks and a slow slip event preceded the 2014 Iquique M_W 8.1 earthquake

S. Ruiz *et al.*

Science **345**, 1165 (2014);
DOI: 10.1126/science.1256074

excluded for SN2014J (*34*). But in this case, the accreted material is mostly He, and the accretion rate can be very high, up to 10^{-4} solar masses per year (*44*). If the white dwarf is rapidly rotating or if mass is accreted faster than it loses angular momentum and thus spreads over the white dwarf, a He belt will be accumulated.

An equatorial ring as inferred here might not be that uncommon. Recently, Hubble Space Telescope imaging of the light echo from the recurrent nova T Pyx revealed a clumpy ring (*45*). Once this belt becomes dense enough, explosive He burning may be ignited, leaving an ejecta configuration as shown in Fig. 3. This may be consistent with the observed gamma-ray and optical signals. Our radiation transfer simulations in UV/optical/near-IR (fig. S10) show that the Ni belt would not produce easily distinguishable features but would result in a normal SN Ia appearance, not only for a pole-on observer but also for an equatorial observer. In view of this, the interpretation of having this type of explosion as a common scenario is not rejected by statistical arguments (see the supplementary materials for more details).

The evolution of the ^{56}Co gamma-ray signal should reveal further aspects of the ^{56}Ni distribution in SN2014J. These lines with associated continua have been recognized to emerge in data from both INTEGRAL instruments (*46*), as more of the total ^{56}Ni produced in the SN becomes visible when the gamma-ray photosphere recedes into the SN interior.

REFERENCES AND NOTES

1. J. Fossey, B. Cooke, G. Pollack, M. Wilde, T. Wright, *Central Bureau Electronic Telegrams No.* **3792** (2014).
2. Y. Cao, M. M. Kasliwal, A. McKay, A. Bradley, *Astronomers Telegram*, no. 5786 (2014).
3. W. Zheng *et al.*, *Astrophys. J. Lett.* **783**, L23 (2014).
4. J. J. Dalcanton *et al.*, *Astrophys. J.* **183** (suppl.), 67–108 (2009).
5. A. Goobar, B. Leibundgut, *Annu. Rev. Nucl. Part. Sci.* **61**, 251–279 (2011).
6. W. Hillebrandt, J. Niemeyer, *Annu. Rev. Astron. Astrophys.* **38**, 191–230 (2000).
7. W. Hillebrandt, M. Kromer, F. K. Röpke, A. J. Ruiter, *Front. Phys.* **8**, 116–143 (2013).
8. W. Li *et al.*, *Nature* **480**, 348–350 (2011).
9. J. F. Guillochon, M. Dan, E. Ramirez-Ruiz, S. Rosswog, *Astrophys. J.* **709**, L64–L69 (2010).
10. S. Rosswog, D. Kasen, J. Guillochon, E. Ramirez-Ruiz, *Astrophys. J. Lett.* **705**, L128–L132 (2009).
11. M. Fink *et al.*, *Astron. Astrophys.* **514**, A53 (2010).
12. R. Pakmor *et al.*, *Astrophys. J.* **747**, L10 (2012).
13. F. K. Röpke *et al.*, *Astrophys. J. Lett.* **750**, L19 (2012).
14. M. C. P. Bours, S. Toonen, G. Nelemans, *Astron. Astrophys.* **552**, A24 (2013).
15. P. Ruiz-Lapuente *et al.*, *Nature* **431**, 1069–1072 (2004).
16. W. E. Kerzendorf *et al.*, *Astrophys. J.* **701**, 1665–1672 (2009).
17. B. E. Schaefer, A. Pagnotta, *Nature* **481**, 164–166 (2012).
18. J. S. Bloom *et al.*, *Astrophys. J. Lett.* **744**, L17 (2012).
19. B. J. Shappee, K. Z. Stanek, R. W. Pogge, P. M. Garnavich, *Astrophys. J.* **762**, L5 (2013).
20. A. Goobar *et al.*, *Astrophys. J.* **784**, L12 (2014).
21. P. Höflich, *Nucl. Phys. A.* **777**, 579–600 (2006).
22. S. A. Sim, P. A. Mazzali, *Mon. Not. R. Astron. Soc.* **385**, 1681 (2008).
23. J. Isern *et al.*, *Astron. Astrophys.* **552**, A97 (2013).
24. A. Summa *et al.*, *Astron. Astrophys.* **554**, A67 (2013).
25. K. Maeda *et al.*, *Astrophys. J.* **760**, 54 (2012).
26. L.-S. The, A. Burrows, *Astrophys. J.* **786**, 141 (2014).
27. C. Winkler *et al.*, *Astron. Astrophys.* **411**, L1–L6 (2003).
28. E. Kuulkers, INTEGRAL Target of Opportunity observations of the type Ia SN2014J in M82. *Astronomers Telegram*, no. 5835 (2014).
29. G. Vedrenne *et al.*, *Astron. Astrophys.* **411**, L63–L70 (2003).
30. J. P. Roques *et al.*, *Astron. Astrophys.* **411**, L91–L100 (2003).
31. T. Siegert, thesis, Technische Universität München, Munich, Germany (2013).
32. R. Diehl *et al.*, *Astron. Astrophys.* **441**, L117 (2003).
33. P. E. Nugent *et al.*, *Nature* **480**, 344–347 (2011).
34. M. T. B. Nielsen, M. Gilfanov, A. Bogdan, T. E. Woods, G. Nelemans, Upper limits on the luminosity of the progenitor of type Ia supernova SN2014J. http://arxiv.org/abs/1402.2896 (2014).
35. P. L. Kelly, *et al.*, http://arxiv.org/abs/1403.4250 (2014).
36. A. J. Ruiter, K. Belczynski, S. A. Sim, I. R. Seitenzahl, D. Kwiatkowski, *Mon. Not. R. Astron. Soc.* **440**, L101–L105 (2014).
37. M. Fink, W. Hillebrandt, F. K. Röpke, *Astron. Astrophys.* **476**, 1133–1143 (2007).
38. R. Moll, S. E. Woosley, *Am. Astron. Soc. Abstr.* **221**, no. 253.22 (2013).
39. M. Kromer *et al.*, *Astrophys. J.* **719**, 1067–1082 (2010).
40. P. Nugent, E. Baron, D. Branch, A. Fisher, P. H. Hauschildt, *Astrophys. J.* **485**, 812–819 (1997).
41. R. Kippenhahn, H. C. Thomas, *Astron. Astrophys.* **63**, 265 (1978).
42. A. L. Piro, L. Bildsten, *Astrophys. J.* **603**, 252–264 (2004).
43. J. Greiner, in *Lecture Notes in Physics* (Springer Verlag, Berlin, 1996), vol. 472, pp. 299–337.
44. W. Y. Law, H. Ritter, *Astron. Astrophys.* **123**, 33–38 (1983).
45. J. L. Sokoloski, A. P. S. Crotts, S. Lawrence, H. Uthas, *Astrophys. J.* **770**, L33 (2013).

ACKNOWLEDGMENTS

This research was supported by the Deutsche Forschungsgemeinschaft (DFG) cluster of excellence "Origin and Structure of the Universe" and from DFG Transregio Project No. 33 "Dark Universe." S.A.G. acknowledges support from the Russian Academy of Sciences, program RAS P-21. F.K.R. was supported by the DFG (Emmy Noether Programm RO3676/1-1) and the ARCHES prize of the German Ministry for Education and Research. The work by K.M. is partly supported by a Japan Society for the Promotion of Science Grant-in-Aid for Scientific Research (grant no. 23740141 and 26800100) and WPI, at the Ministry of Education, Culture, Sports. Science & Technology. We are grateful to E. Kuulkers for handling the observations and to X. Zhang for preparing our SPI data for the INTEGRAL SN2014J campaign. The INTEGRAL/SPI project has been completed under the responsibility and leadership of CNES Toulouse. We are grateful to the agencies and institutions of ASI, CEA, CNES, DLR, ESA, INTA, NASA, and OSTC for support of this ESA space science mission. INTEGRAL's data archive (http://www.isdc.unige.ch/integral/archive#DataRelease) is at the INTEGRAL Science Data Center in Versoix, Switzerland, and includes the SN2014J data used in this paper.

SUPPLEMENTARY MATERIALS

www.sciencemag.org/content/345/6201/1162/suppl/DC1
Materials and Methods
Supplementary Text
Figs. S1 to S10
Tables S1 and S2
References (*46*–*58*)

14 April 2014; accepted 21 July 2014
Published online 31 July 2014;
10.1126/science.1254738

EARTHQUAKE DYNAMICS

Intense foreshocks and a slow slip event preceded the 2014 Iquique M_w 8.1 earthquake

S. Ruiz,[1]* M. Metois,[2] A. Fuenzalida,[3] J. Ruiz,[1] F. Leyton,[4] R. Grandin,[5] C. Vigny,[6] R. Madariaga,[6] J. Campos[1]

The subduction zone in northern Chile is a well-identified seismic gap that last ruptured in 1877. The moment magnitude (M_w) 8.1 Iquique earthquake of 1 April 2014 broke a highly coupled portion of this gap. To understand the seismicity preceding this event, we studied the location and mechanisms of the foreshocks and computed Global Positioning System (GPS) time series at stations located on shore. Seismicity off the coast of Iquique started to increase in January 2014. After 16 March, several $M_w > 6$ events occurred near the low-coupled zone. These events migrated northward for ~50 kilometers until the 1 April earthquake occurred. On 16 March, on-shore continuous GPS stations detected a westward motion that we model as a slow slip event situated in the same area where the mainshock occurred.

Since the giant moment magnitude (M_w) 8.8 megathrust earthquake of 1877 (*1*–*4*), the ≥500-km-long region stretching from Arica (18°S) to the Mejillones Peninsula of Chile (24.5°S) (Fig. 1) has had relatively few major seismic events, with only moderate $M_w < 8$ events in 1933, 1967, and 2007 (*4*–*9*). On the basis of recent geodetic data (*5*, *10*, *11*), the degree of interseismic coupling (that is, the ratio between the interseismic slip rate and the plate-convergence velocity) in the area shows two distinct highly coupled segments (Loa and Camarones) separated by a low-coupling zone (LCZ) off the coast of Iquique (*5*). On 1 April 2014, a ~150-km-long portion of the gap broke in a M_w 8.1 earthquake after a strong precursory activity that started on 16 March (*12*, *13*). Understanding the complex nucleation phase

[1]Departamento de Geofísica, Facultad de Ciencias Físicas y Matemáticas, Universidad de Chile, Santiago, Chile. [2]Istituto Nazionale di Geofisica e Vulcanologia, Centro Nazionale Terremoti, Rome, Italy. [3]School of Environmental Sciences, University of Liverpool, Liverpool, UK. [4]Centro Sismológico Nacional, Facultad de Ciencias Físicas y Matemáticas, Universidad de Chile, Santiago, Chile. [5]Institut de Physique du Globe de Paris, Sorbonne Paris Cité, Université Paris Diderot, UMR 7154 CNRS, Paris, France. [6]Laboratoire de Geologie, UMR 8538 CNRS Ecole Normale Superieure, Paris, France.
***Corresponding author. E-mail: sruiz@dgf.uchile.cl**

preceding the M_w 8.1 mainshock and its coseismic rupture should provide insights into the seismic gap history, present-day seismic hazard, and nucleation process of megathrust earthquakes.

Seismic activity preceding the Iquique earthquake initiated in a region between 19.5°S and 21°S, where coupling ranges from 0.2 to 0.5 (*5*); that is, the plates are slowly creeping past each other at a fraction of the plate rate (when the plates are fully locked, coupling is 1.0). This region was actively monitored because its seismic activity had steadily increased since 2008,

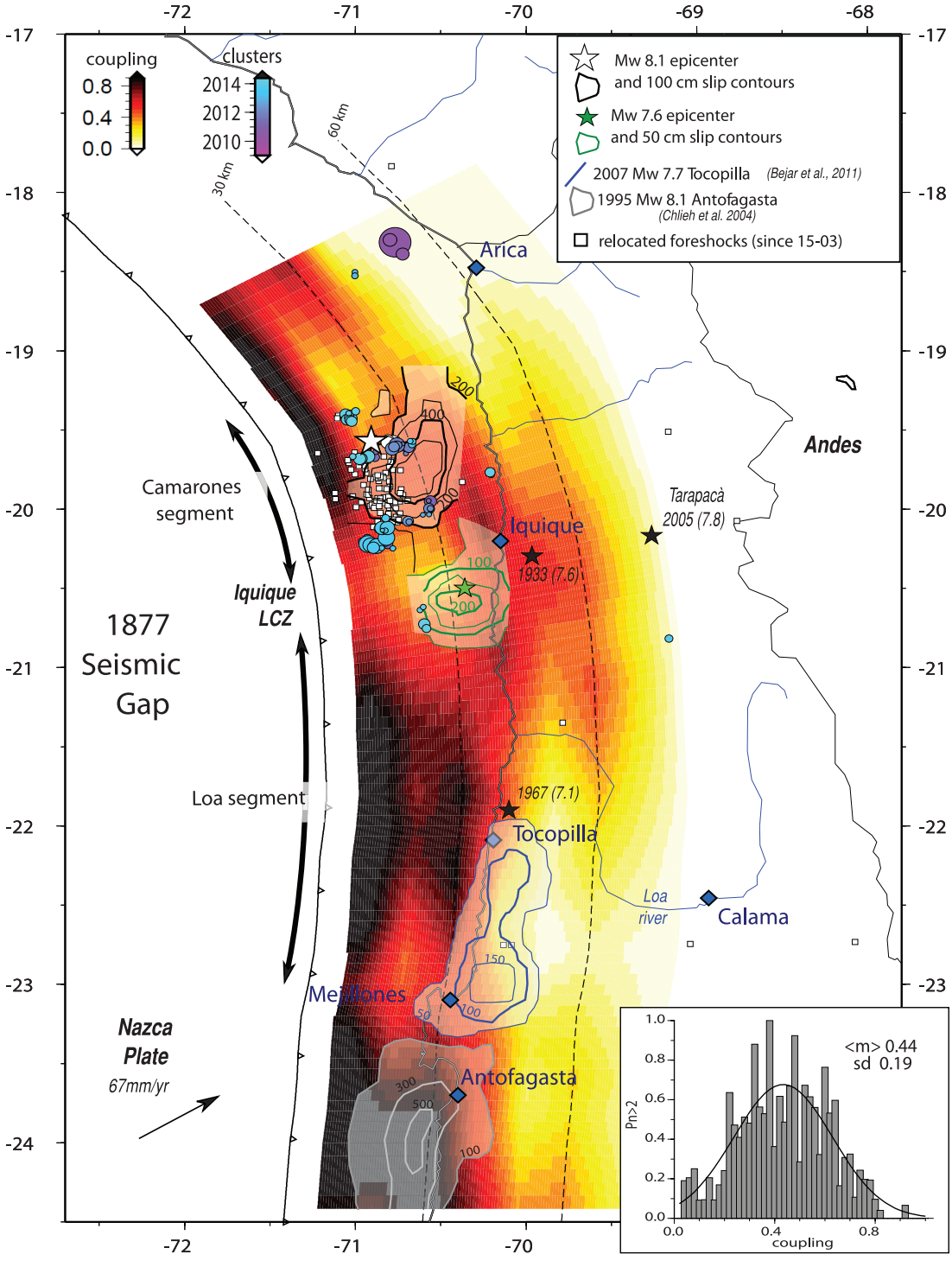

Fig. 1. Northern Chile seismic gap. Interseismic coupling was calculated from GPS measurements acquired in the zone since 2008. Slip contours are shown with continuous lines for the 2007 M_w 7.7 Tocopilla, 1995 M_w 8.0 Antofagasta, and 2014 M_w 8.1 and 7.6 Iquique earthquakes. Precursory seismicity from January to March 2014 is shown with light blue circles. Foreshocks from March 2014 are shown with open squares. The dashed lines denote the surface projection of the subduction interface isodepths. (**Inset**) Normalized probability that two or more $M_w < 7$ earthquakes occurred since 2008 (CSN catalog) as a function of the value of interseismic coupling. The upper right corner indicates the mean and standard deviation of the best-fit normal distribution.

with repeated interplate thrust events of magnitude <4.0. Several seismic clusters were located in this region by the National Seismological Center of Chile (CSN) (Fig. 1 and fig. S1); some of these clusters were associated with persistent microseismicity observed by the nearest seismological stations (fig. S2). Global catalogs reveal an increase in seismicity near Iquique since 2005, compared with the previous 10 years (fig. S3). To understand the seismicity that preceded the 1 April mainshock, we used the events listed in the CSN catalog to relocalize and estimate the focal mechanism of several foreshocks of this sequence. Simultaneously, we calculated the Global Positioning System (GPS) time series of the closest permanent stations up to the date of the mainshock and inverted for the slip rate on the plate interface (*14*).

The most recent seismic activity in northern Chile started on 4 January 2014, when a M_w 5.7 interplate thrust event took place at 20.69°S, 70.80°W on the southern edge of the Iquique LCZ (*5*). On 8 January, another M_w 5.7 event occurred in the same area. The automatic location system of CSN identified 30 events in a smaller region of 15 km by 15 km, in the period from 4 to 24 January 2014. Then on 12 January, a small cluster of six identified events occurred north of the previous ones at (19.7°S, 71.0°W). During February 2014, another small cluster occurred near 19.4°S, 71.0°W, where 16 events with local magnitude (ML) 2.4 to 4.0 were identified (Fig. 1, fig. S4, and table S1). On 15 March, the area was reactivated with 11 events of ML 2.6 to 4.6, followed on 16 March by the first big foreshock of M_w 6.7, ~50 km south and with a slightly deeper centroid (fig. S4). This event triggered a persistent precursory seismicity, including a M_w 6.3 earthquake on 22 March, which slowly moved northward and lasted until the occurrence of the 1 April 2014 M_w 8.1 event (Fig. 2 and fig. S4).

Overall, these foreshocks delineate a region that spans ~150 km along the strike of the subduction zone. We relocated this precursory seismicity and computed regional seismic moment tensor using a linear time-domain, broadband waveform inverse method (*15*) (Fig. 2). The centroid of the M_w 6.7 precursor of 16 March was only 10 km deep, in an area where the seismogenic interface is at a depth of ~20 km (*16*) (Fig. 2 and fig. S5). This event had a reverse focal mechanism with a strike of 277° that is at a sharp angle with respect to the trench (Fig. 2A). Over the course of 1 week, a persistent seismicity occurred in a zone of 10-km radius (Fig. 2C); most of these events were located inside the shallow South American plate and had very diverse focal mechanisms. On 22 March, a new M_w 6.3 foreshock occurred ~30 km north of the 16 March foreshock. After this event, precursory seismicity moved to the vicinity of the 22 March foreshock with depths and mechanisms indicating that it occurred at the plate interface (Fig. 2B).

From 16 March until the 1 April mainshock (i.e., for 17 days), all of the continuous GPS (cGPS) stations located along the coast between Iquique and Pisagua started to move trenchward (Fig. 3). This slowly increasing westward motion is in contrast to the usual inland-directed interseismic motion. The displacements measured during this period were quite large (>5 mm for the stations located between Iquique and Pisagua and ~1 cm at the PSGA station). Only a fraction of this cumulative displacement (up to 20%) can be attributed to the largest foreshock of 16 March (M_w 6.7), suggesting that slow aseismic slip was taking place offshore, concurrently with the development of the precursory seismicity. Whether this motion started slightly before or coincided with the 16 March foreshock is beyond the current GPS resolution. We inverted for the slip distributions on the subduction interface that best reproduce the observed displacements using Okada's formulas for an elastic half-space (*14*) (Fig. 4). We found a slip of ~0.8 m for the M_w 6.7 events of 16 March, located in a narrow area

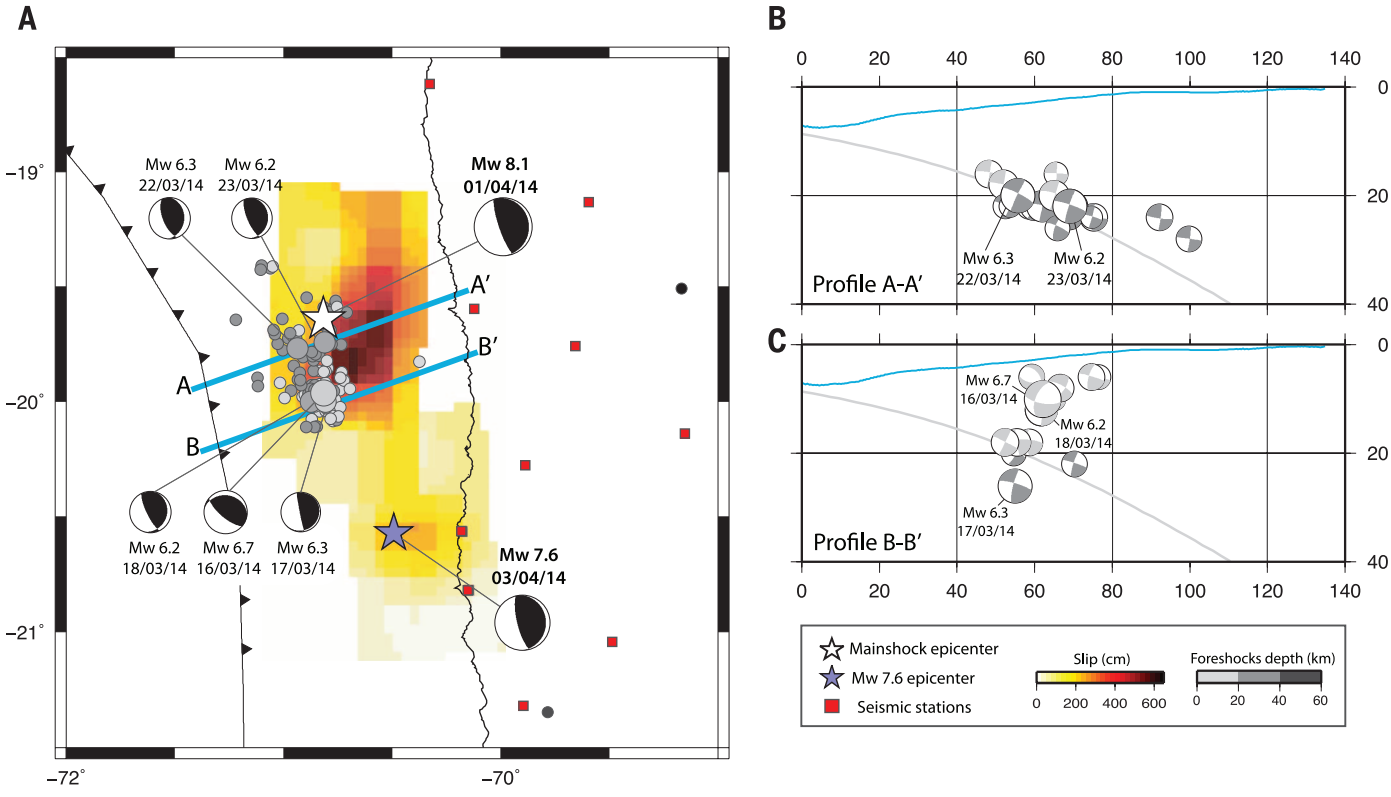

Fig. 2. Seismicity preceding the Iquique earthquake. (**A**) Gray dots show the foreshocks from 16 to 31 March; the intensity of the gray color indicates the depths of the events. The slip distribution of the M_w 8.1 and M_w 7.6 earthquakes inverted from far-field broadband records of the International Federation of Digital Seismograph Networks is shown with the color. (**B**) A 15-km-wide cross section along the A-A′ line shown in (A). (**C**) A 15-km-wide cross section along the B-B′ line shown in (A). In the vertical cross sections, we plot the focal mechanisms of events with M_w > 4.6. Mechanisms were computed by broadband moment tensor analysis. The gray curve shows the seismogenic contact according to (*16*).

in the vicinity of the CSN epicenter. We then computed the aseismic slip for the period from 10 March to the mainshock that extends over an area of 70 km by 20 km located between the foreshocks and the coast (Fig. 4).

The 1 April 2014 Iquique earthquake started with a small shock at the northern end of the region activated by the precursors that occurred in March (19.57°S, 70.91°W). The peak seismic moment release rate during the M_w 8.1 earthquake took place ~30 s after the initial nucleation (fig. S6). We used standard teleseismic methods (*17*) to invert for the coseismic slip of the main event and its large M_w 7.6 aftershock that occurred 2 days later (Fig. 2 and figs. S6 and S7). The maximum slip associated with these events was deeper than that of the March precursors and ~20 km inland, affecting areas of higher coupling (>0.6). Coseismic slip appears to overlap (at least partially) with the slow slip event (SSE) (Fig. 4), but no substantial coseismic slip occurred in the LCZ (Fig. 1). Whereas precursory seismicity migrated northward, the mainshock and its aftershock propagated toward the south, similar to what was observed for the 2007 M_w 7.8 Tocopilla earthquake (*7*, *8*).

The LCZ off the coast of Iquique can be assumed to play a key role in the events that occurred in northern Chile during, and in the 20 years preceding, this precursory sequence. The seismic swarms detected since 2008 occurred on the edges of the LCZ, and most moderate seismicity took place preferentially in zones of intermediate coupling (see inset in Fig. 1 and fig. S8), suggesting that aseismic creep occurring on the LCZ triggered seismic activity in its vicinity. Up to now, SSEs have remained undetected by the cGPS network operating in northern Chile for more than a decade. Nevertheless, the very inference of a LCZ off the coast of Iquique implies some degree of accommodation of plate convergence by aseismic slip, which might operate by repeated SSEs. We postulate that until now, either the magnitude of these SSEs was too small, or they occurred too far from the coast to be detected by GPS measurements. The only major change we detected in plate convergence in the area before 2014 was a long-term velocity change at the cGPS station operating in Iquique since 1995 (UAPE): its eastward velocity decreased after 2005 by ~20%, from 19.5 to 15.2 mm/year (fig. S9). This suggests that interseismic loading has been decreasing in the Iquique area during the past decade, probably reflecting a very SSE occurring on the decadal scale. This change could have been triggered by the deep intraslab 2005 M_w 7.7 Tarapacá earthquake that generated little postseismic relaxation (fig. S9).

Together with the fact that the M_w 8.1 mainshock and M_w 7.6 aftershock ruptures did not penetrate into the LCZ, the foreshock sequence and slow slip preceding the M_w 8.1 event argue for a creeping Iquique LCZ. Because SSEs are often associated with seismic swarms (*18*), we propose that the seismicity observed in northern Chile since 2008 was triggered by a SSE, developing for several years and accelerating during the final foreshock sequence as in the preslip model of nucleation (*19*). As suggested by many laboratory experiments (*20*), the SSE might have occurred in the nucleation zone of the impending megathrust rupture (Fig. 4). This precursory sequence included several shallow crustal events that took place near the 16 March foreshock; these events may be associated with the activation of a listric fault in the outermost fore-arc. This area is poorly known due to the lack of marine seismic profiles, but it may be similar to the eroded wedge enhanced by fracturing imaged at 22°S (*21*).

Several other subduction earthquakes were preceded by precursory seismic activity (*12*); in particular, the 1985 Valparaiso M_w 8.0 (*22*) and 2010 Maule M_w 8.8 (*23*) Chilean events and the

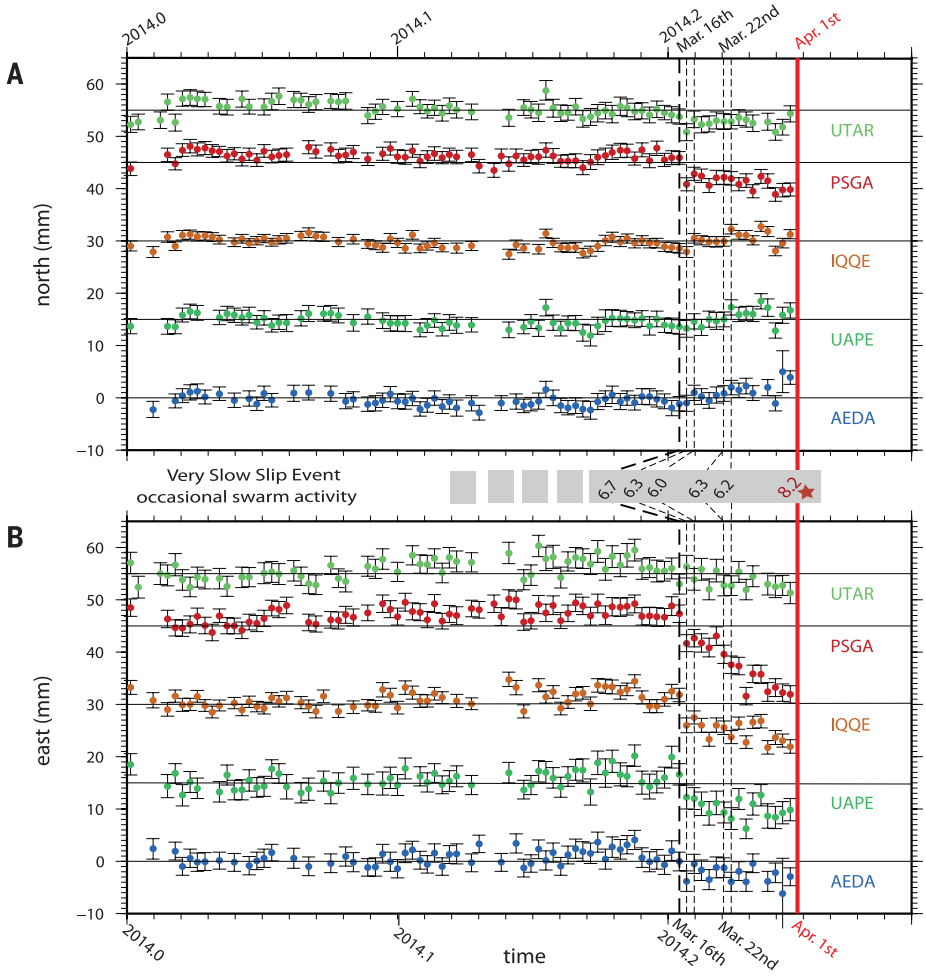

Fig. 3. Motion of coastal GPS stations preceding the Iquique earthquake. (**A**) North and (**B**) east components relative to a linear evolution model with seasonal variations estimated since 2012 (*14*). The thick red line denotes the origin time of the mainshock, whereas the black dotted lines show the occurrence times of the M_w > 6 foreshocks. Error bars indicate 1σ formal uncertainty.

2011 Tohoku-Oki earthquake (*24*). However, the size and duration of the precursory events of the 1 April mainshock are distinct. The occurrence of a SSE before the 2011 M_w 9.0 Tohoku-Oki earthquake and possibly the 2001 M_w 8.4 Arequipa earthquake (*24*, *25*) implies that SSE may be a common precursory feature and a potential triggering mechanism for large megathrust ruptures.

On the other hand, whether the shallowest part of the Camarones segment is still coupled and capable of producing a large earthquake or creeping aseismically is beyond the current resolution of the GPS network. The large aftershock of 3 April left the highly coupled Loa segment south of Iquique largely untouched. Several earthquakes of equivalent or larger magnitude may still rupture the deep intermediate-coupling areas of this segment.

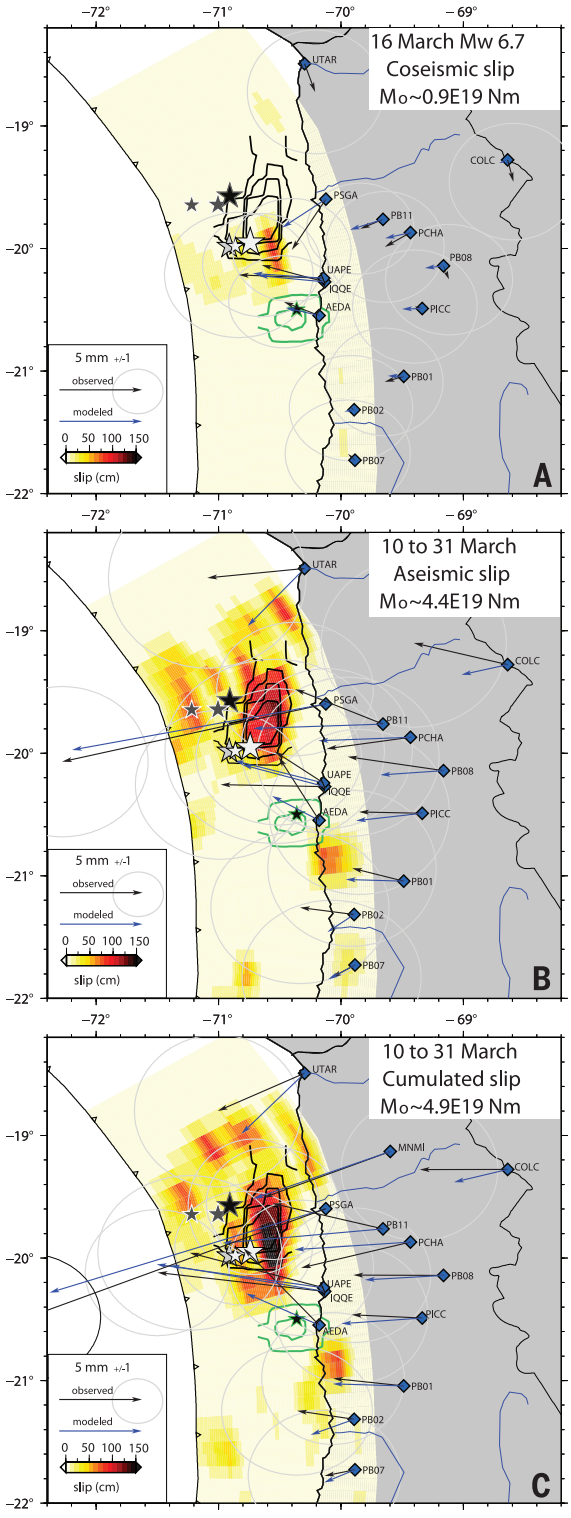

Fig. 4. Slip distribution preceding the Iquique earthquake. The slip distributions were inverted using Okada's equations for an elastic half-space from the surface displacements observed during the preseismic phase (*14*) (Fig. 3). (**A**) Coseismic slip due to the 16 March M_w 6.7 earthquake. (**B**) Aseismic slip for the period ranging from 10 to 31 March 2014. (**C**) Cumulative slip model for displacements observed from 10 to 31 March 2014. Black and green contours are the slip distributions for the mainshock and the main aftershock, respectively, already presented in Fig. 2. Mo, seismic moment.

REFERENCES AND NOTES

1. F. Montessus de Ballore, *Historia Sísmica de los Andes Meridionales* (Editorial Cervantes, Santiago, 1916).
2. E. Kausel, *Bol. Acad. Chil. Ciencias* **3**, 8–12 (1986).
3. C. Lomnitz, *Geofis. Panamericana* **1**, 151–178 (1971).
4. D. Comte, M. Pardo, *Nat. Hazards* **4**, 23–44 (1991).
5. M. Metois *et al*., *Geophys. J. Int.* **194**, 1283–1294 (2013).
6. M. Malgrange, R. Madariaga, *Geophys. J. R. Astron. Soc.* **73**, 489–505 (1983).
7. S. Peyrat *et al*., *Geophys. J. Int.* **182**, 1411–1430 (2010).
8. A. Fuenzalida, B. Schurr, M. Lancieri, M. Sobiesiak, R. Madariaga, *Geophys. J. Int.* **194**, 1216–1238 (2013).
9. E. R. Engdahl, A. Villaseñor, in *International Handbook of Earthquake and Engineering Seismology* (Academic Press, San Diego, 2002), part A, chap. 41.
10. M. Chlieh *et al*., *J. Geophys. Res.* **116**, B12405 (2011).
11. M. Béjar-Pizarro *et al*., *Nat. Geosci.* **6**, 462–467 (2013).
12. Th. Lay, H. Yue, E. Brodsky, C. An, *Geophys. Res. Lett.* **41**, 3818–3825 (2014).
13. Y. Yagi *et al*., *Geophys. Res. Lett.* **41**, 4201–4206 (2014).
14. Materials and methods are available as supplementary materials on *Science* Online.
15. M. E. Pasyanos, D. S. Dreger, B. Romanowicz, *Bull. Seismol. Soc. Am.* **86**, 1255–1269 (1996).
16. G. Hayes, D. J. Wald, R. L. Johnson, *J. Geophys. Res.* **117**, B01302 (2012).
17. M. Kikuchi, H. Kanamori, *Bull. Seismol. Soc. Am.* **81**, 2335–2350 (1991).
18. S. Ozawa, H. Suito, M. Tobita, *Earth Planets Space* **59**, 1241–1245 (2007).
19. W. L. Ellsworth, G. C. Beroza, *Science* **268**, 851–855 (1995).
20. S. Latour, A. Schubnel, S. Nielsen, R. Madariaga, S. Vinciguerra, *Geophys. Res. Lett.* **40**, 5064–5069 (2013).
21. E. Contreras-Reyes, J. Jara, I. Grevemayer, S. Ruiz, D. Carrizo, *Nat. Geosci.* **5**, 342–345 (2012).
22. D. Comte *et al*., *Science* **233**, 449–453 (1986).
23. R. Madariaga, M. Métois, C. Vigny, J. Campos, *Science* **328**, 181–182 (2010).
24. A. Kato *et al*., *Science* **335**, 705–708 (2012).
25. J. C. Ruegg, M. Olcay, D. Lazo, *Seismol. Res. Lett.* **72**, 673–678 (2001).

ACKNOWLEDGMENTS

We thank J. C. Ruegg for his initiative to study northern Chile with GPS, followed by J. B. De Chabalier, A. Socquet, D. Carrizo, and others after him. S.R., J.R., R.M., and J.C. acknowledge the support of the Chilean National Science Foundation project FONDECYT no.1130636 and S.R. of project FONDECYT no.11130230. This work received partial support from ANR-2011-BS56-017 and ANR-2012-BS06-004 of the French Agence Nationale de la Recherche. This is Institut de Physique du Globe de Paris contribution no. 3551. We thank Incorporated Research Institutions for Seismology Data Management Center (www.iris.edu/data/), International Plate Boundary Observatory Chile (http://geofon.gfz-potsdam.de/waveform/), Centro Sismológico Nacional (www.sismologia.cl), and International Associated Laboratory Montessus de Ballore for making raw data available to us.

SUPPLEMENTARY MATERIALS

www.sciencemag.org/content/345/6201/1165/suppl/DC1
Materials and Methods
Figs. S1 to S13
Tables S1 and S2
References (*26*–*32*)

14 May 2014; accepted 15 July 2014
Published online 24 July 2014;
10.1126/science.1256074